New Journal of Physics
The open access journal at the forefront of physics

Deutsche Physikalische Gesellschaft DPG
IOP Institute of Physics

Published in partnership with: Deutsche Physikalische Gesellschaft and the Institute of Physics

OPEN ACCESS

RECEIVED
27 February 2017

REVISED
13 June 2017

ACCEPTED FOR PUBLICATION
15 June 2017

PUBLISHED
8 August 2017

PAPER

Full-counting statistics of energy transport of molecular junctions in the polaronic regime

Gaomin Tang[1,2], **Zhizhou Yu**[1,2,3] **and Jian Wang**[1,2]

[1] Department of Physics and the Center of Theoretical and Computational Physics, The University of Hong Kong, Hong Kong, People's Republic of China
[2] The University of Hong Kong Shenzhen Institute of Research and Innovation, Shenzhen, People's Republic of China
[3] School of Physics and Technology, Nanjing Normal University, Nanjing 210023, People's Republic of China

E-mail: jianwang@hku.hk

Keywords: molecular junctions, full-counting statistics, nonequilibrium energy transport, polaronic regime, nonequilibrium Green's function

Abstract

We investigate the full-counting statistics (FCS) of energy transport carried by electrons in molecular junctions for the Anderson–Holstein model in the polaronic regime. Using the two-time quantum measurement scheme, the generating function (GF) for the energy transport is derived and expressed as a Fredholm determinant in terms of Keldysh nonequilibrium Green's function in the time domain. Dressed tunneling approximation is used in decoupling the phonon cloud operator in the polaronic regime. This formalism enables us to analyze the time evolution of energy transport dynamics after a sudden switch-on of the coupling between the dot and the leads towards the stationary state. The steady state energy current cumulant GF in the long time limit is obtained in the energy domain as well. Universal relations for steady state energy current FCS are derived under a finite temperature gradient with zero bias and this enabled us to express the equilibrium energy current cumulant by a linear combination of lower order cumulants. The behaviors of energy current cumulants in steady state under temperature gradient and external bias are numerically studied and explained. The transient dynamics of energy current cumulants is numerically calculated and analyzed. Universal scaling of normalized transient energy cumulants is found under both temperature gradient and external bias.

1. Introduction

Rapid experimental development in the field of nanotechnology makes fabrication of single-molecule junctions possible [1, 2], which could push the limit of Moore's law further. In the electronic quantum transport though nano-devices, the electron–phonon coupling plays an important role. One of the mechanisms that induces electron–phonon coupling is due to the charging of the molecule leading to elastic mechanical deformations. This in turn causes an interaction between the electronic and quantized mechanical degrees of freedom giving rise to electron–phonon coupling. A variety of intriguing transport properties, such as phonon-assisted current steps and Franck–Condon blockade [5], have been found in the polaronic regime [3, 4] when this kind of electron–phonon coupling in molecular junctions is strong. Theoretically, these phenomena could be understood using a quantum dot described by the Anderson–Holstein model [6, 7] coupled to two electrodes.

To understand quantum transport in the polaronic regime, many methods have been used, such as the master equation method [8–11], diagrammatic quantum Monte Carlo method [12], numerical renormalization group method [13], as well as the nonequilibrium Green's function (NEGF) technique [20] that is particularly useful in describing time dependent nonequilibrium processes. The perturbation method is applicable when the electron–phonon coupling strength is weak [14–16] and it fails in the strong electron–phonon coupling system. Other approximation has to be made in order to deal with the strong and intrinsically nonlinear electron–phonon interaction in the Anderson–Holstein model. In order to decouple the phonon cloud operator in the

polaronic regime, dressed tunneling approximation (DTA), in which the leads' self-energies are dressed with the polaronic cloud, has been proposed to eliminate the noticeable pathological features of the single particle approximation (SPA) at low frequencies and polaron tunneling approximation (PTA) at high frequencies [17–20].

It is known that quantum transport is determined in nature by stochastic process which can be characterized by the corresponding distribution function [21]. The study of full-counting statistics (FCS) pioneered by Levitov and Lesovik [22–24] could provide us with a full view of the probability distribution of electron and energy transport [18–20, 25–36]. The key in FCS is to obtain the generating function (GF) which is actually the Fourier transform of the probability distribution of the related physical quantity. Using the NEGF technique [37–40] and the path integral method under the two-time quantum measurement scheme [27, 41–43], GF was formulated as a Fredholm determinant in the time domain for both phonon [29–31] and electron [27, 32–35] transport. This formalism enables one to study the transport properties in the transient regime providing more information on the short time dynamics [32]. Recently the transient dynamics of particle current transport in the molecular junctions was studied by Schmidt *et al* [44, 45] in the case of weak and strong electron–phonon couplings and has been reported by Maier *et al* using PTA [46] and by Souto *et al* using DTA [20] in the polaronic regime.

The transport study of energy flow in the nonequilibrium system could reveal information on how energy is dissipated and its correlation for electronic devices and can be investigated theoretically by the Landauer–Büttiker type of formalism for noninteracting systems [47–49]. Energy transport in trapped ion chains has been measured experimentally by Ramm *et al* [50]. The heat current I_α^h in the α lead is related to the energy current I_α^E by the expression $I_\alpha^h = I_\alpha^E - \mu_\alpha I_\alpha$ with the particle current I_α and the chemical potential μ_α in the α lead, and this quantity is quite important in characterizing the efficiency of thermoelectric devices [51]. So far, the FCS of energy transfer mostly focuses on phonon transport both in the transient regime and steady states [29–31] and less attention has been paid to the FCS of energy transfer carried by electrons in electronic transport problems. In our previous work, we investigated the transient FCS of energy transfer in the noninteracting system [34]. It would be important and interesting to study the FCS of energy transport carried by electrons of molecular junctions with electron–phonon coupling in the polaronic regime for both transient dynamics and steady states, and this is the purpose of this work.

In this paper, the FCS of energy transport carried by electrons in molecular junctions for the Anderson–Holstein model in the polaronic regime is investigated both in the steady states and transient regime. Within the DTA, the GF for the energy current is derived from the equation of motion and can be expressed as a Fredholm determinant in the time domain using NEGF. Numerical calculation is performed which allows us to analyze the time evolution of the energy flow towards the steady state for a sudden switch-on of the coupling between the quantum dot and the leads. The cumulant GF of energy current in the steady state is obtained analytically in the energy domain. Universal relations for cumulants of energy current under a finite temperature gradient with zero voltage bias are established. In addition, we also calculate and analyze the steady state solution for various orders of cumulants (from the first to the fourth order) under temperature gradient or external bias.

The remainder of the paper is organized as follows. In section 2, the model Hamiltonian of a molecular junction is introduced and GF of energy flow in the transient regime is determined in terms of NEGF in the time domain. Section 3 is devoted to the steady state investigation of the FCS of energy current, both theoretically and numerically. In section 4, the transient dynamics of energy current is investigated under a sudden switching-on of external bias. Finally, a brief conclusion is given in section 5.

2. Model and basic theoretical formalism

Considering only the lowest electronic orbital, the single-molecule is simplified as a single electronic level of a quantum dot (QD) being coupled to localized vibrational mode, which is the simplest spinless Anderson–Holstein model [52]. The QD then is coupled to the left and right electrode so that the system is driven to a nonequilibrium state when the external bias or temperature gradient is applied (figure 1). The corresponding Hamiltonian reads as

$$H = H_{\rm S} + H_{\rm L} + H_{\rm R} + H_{\rm T} \tag{1}$$

with the Hamiltonian of the central dot (in natural units, $\hbar = k_B = e = m_e = 1$)

$$H_{\rm S} = \epsilon_0 d^\dagger d + \omega_0 a^\dagger a + t_{ep}(a^\dagger + a) d^\dagger d, \tag{2}$$

where ϵ_0 is the bare electronic energy level, and ω_0 is the frequency of the localized vibron. $d^\dagger$ ($a^\dagger$) denotes the electron (phonon) creation operator in the QD. The localized vibron modulates the QD with the electron–phonon coupling constant t_{ep}. The Hamiltonians of the leads is given in a compact form

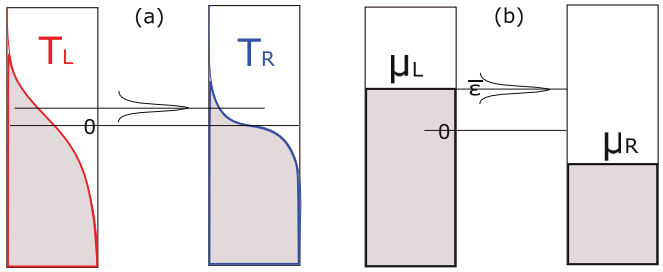

Figure 1. Sketch of a QD coupled to the left and right lead under (a) temperature gradient $T_{\rm L} > T_{\rm R}$ with zero chemical potentials in both leads and (b) external bias $\Delta\mu$ with $\mu_{\rm L(R)} = \pm\Delta\mu/2$ under zero temperature.

$$H_\alpha = \sum_{x\in k\alpha} \epsilon_x c_x^\dagger c_x, \tag{3}$$

where the indices $k\alpha = k$L, kR are used to label the different states in the left and right leads. $H_{\rm T}$ is the Hamiltonian describing the coupling between the dot and the leads with the tunneling amplitudes $t_{k\alpha}$,

$$H_{\rm T} = H_{\rm LS} + H_{\rm RS} = \sum_{k\alpha}(t_{k\alpha} c_{k\alpha}^\dagger d + t_{k\alpha}^* d^\dagger c_{k\alpha}). \tag{4}$$

The tunneling rate (linewidth function) of lead α is assumed to bear the Lorentzian form and can be expressed as

$$\mathbf{\Gamma}_\alpha(\omega) = {\rm Im}\sum_k \frac{|t_{k\alpha}|^2}{\omega - \epsilon_{k\alpha} - i0^+} = \frac{\Gamma_\alpha W^2}{\omega^2 + W^2}, \tag{5}$$

with the linewidth amplitude Γ_α and bandwidth W, and one can denote $\Gamma = \Gamma_{\rm L} + \Gamma_{\rm R}$.

The electron–vibron coupling term can be eliminated by applying the Lang–Firsov unitary transformation [53] given by

$$\bar{H} = SHS^\dagger,\ \ {\rm S} = e^{gd^\dagger d(a^\dagger - a)},\ \ g = \frac{t_{ep}}{\omega_0}, \tag{6}$$

which leads to

$$\bar{H}_{\rm S} = \bar{\epsilon} d^\dagger d + \omega_0 a^\dagger a, \tag{7}$$

where the bare QD electron energy is changed to $\bar{\epsilon} = \epsilon_0 - g^2\omega_0$. The tunneling Hamiltonian is transformed as

$$\bar{H}_{\rm T} = \sum_{k\alpha}(t_{k\alpha} c_{k\alpha}^\dagger X d + t_{k\alpha}^* d^\dagger X^\dagger c_{k\alpha}) \tag{8}$$

with the phonon cloud operator $X = \exp[g(a - a^\dagger)]$, while the Hamiltonians of the isolated leads remain unchanged.

In the present work we study the transient dynamics in which the interaction between the leads and the QD is suddenly turned on at $t = 0$ and afterwards the system evolves to the steady states. The turning on process could be facilitated by a quantum point contact which is controlled by a gate voltage. The initial density matrix of the whole system at $t = 0$ is the direct product of each subsystem and expressed by $\rho(0) = \rho_{\rm L} \otimes \rho_{\rm S} \otimes \rho_{\rm R}$. The statistical behaviors of the energy current in a specific lead are all encoded in the probability distribution $P(\Delta\epsilon,\ t)$ of the transferred energy carried by electrons $\Delta\epsilon = \epsilon_t - \epsilon_0$ between an initial time $t = 0$ and a later time t. The GF $Z(\lambda,\ t)$ with the counting field λ is defined as,

$$Z(\lambda,\ t) \equiv \langle e^{i\lambda\Delta\epsilon}\rangle = \int P(\Delta\epsilon,\ t) e^{i\lambda\Delta\epsilon} d\Delta\epsilon. \tag{9}$$

The kth cumulant of transferred energy $\langle\langle(\Delta\epsilon)^k\rangle\rangle$ can be calculated by taking the kth derivative of cumulant generating function (CGF) which is $\ln Z(\lambda)$ with respect to $i\lambda$,

$$C_k(t) \equiv \langle\langle(\Delta\epsilon)^k\rangle\rangle = \frac{\partial^k \ln Z(\lambda)}{\partial(i\lambda)^k}\bigg|_{\lambda=0}. \tag{10}$$

One can further define the energy current cumulants

$$\langle\langle(I^E)^k\rangle\rangle = \frac{\partial C_k(t)}{\partial t}, \tag{11}$$

which tend to the steady state energy current cumulants in the long time limit $t \to \infty$. The second energy cumulant can be expressed as $C_2(t) = \int_0^t dt_1 \int_0^t dt_2 \langle\delta I^E(t_1)\delta I^E(t_2)\rangle$, so that the second energy current cumulant is $\langle\langle(I^E)^2\rangle\rangle = \frac{1}{2}\int_0^t dt_1\langle\delta I^E(t_1)\delta I^E(t)\rangle + \frac{1}{2}\int_0^t dt_2\langle\delta I^E(t)\delta I^E(t_2)\rangle$. One should note that the second

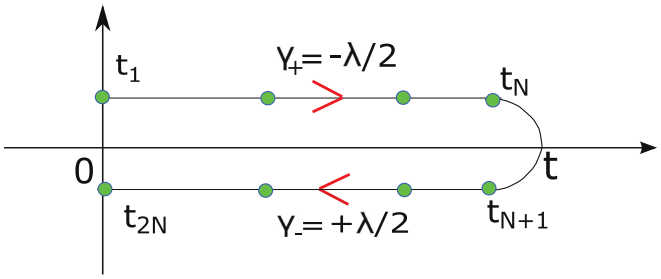

Figure 2. Keldysh contour starting from $t=0$. $\gamma = \pm\lambda/2$ depends on the branch of the contour in which it resides.

energy current cumulant $\langle\langle (I^E)^2\rangle\rangle$ is not an average of a squared quantity. To investigate the statistical behaviors of the energy current through the left lead, we could focus on the energy operator which is actually the free Hamiltonian of the left lead $H_{\rm L}$. Under the two-time measurement scheme, GF of transferred energy in the left lead can be expressed over the Keldysh contour as [27, 31, 33],

$$Z(\lambda, t) = \mathrm{Tr}\left\{\rho(0)\mathcal{T}_C \exp\left[-\frac{i}{\hbar}\int_C H_\gamma(t')dt'\right]\right\} = \mathrm{Tr}\left\{\rho(0)U^\dagger_{\lambda/2}(t,0)U_{-\lambda/2}(t,0)\right\}, \tag{12}$$

with the modified evolution operator ($\gamma = \pm\lambda/2$ depending on the branch of the contour, see figure 2),

$$U_\gamma(t,0) = \mathcal{T}\exp\left[-\frac{i}{\hbar}\int_0^t H_\gamma(t')dt'\right]. \tag{13}$$

Here the modified evolution operator is expressed by the modified Hamiltonian,

$$H_\gamma = \bar{H}_{\rm S} + \sum_k [\epsilon_{k\rm L} c^\dagger_{k\rm L}(t_\gamma)c_{k\rm L}(t_\gamma) + \epsilon_{k\rm R}c^\dagger_{k\rm R}c_{k\rm R}] + \sum_k [(t_{k\rm L}c^\dagger_{k\rm L}(t_\gamma)Xd + t_{k\rm R}c^\dagger_{k\rm R}Xd) + \mathrm{H.c.}], \tag{14}$$

with $t_\gamma = \hbar\gamma$, and $c_{k\rm L}(t_\gamma) = e^{i\gamma H_{\rm L}}c_{k\rm L}(0)e^{-i\gamma H_{\rm L}}$.

The GF for the transferred charges in the transient regime has been expressed by NEGF in the time domain for the noninteracting case [33] and in the polaronic regime using the DTA [18, 20]. GF for the energy current has expressed by NEGF and higher-order cumulants has been investigated by Yu *et al* for the noninteracting case [34]. We now generalize the GF for the transferred energy to the interacting case in the polaronic regime following the derivation of the GF for transferred charges [20]. Following the procedure outlined in [54], one can get GF from the derivative of the logarithm of equation (12) with respect to the counting field,

$$\frac{\partial \ln Z}{\partial\lambda} = \int_C dt' \sum_k \langle \mathcal{T}_C(t_{k\rm L}c^\dagger_{k\rm L}(t' \mp \hbar\lambda/2)X(t')d(t') - t^*_{k\rm L}d^\dagger(t')X^\dagger(t')c_{k\rm L}(t' \pm \hbar\lambda/2))\rangle, \tag{15}$$

where we take ' $-$ ' in the first part and ' $+$ ' in the second for the forward time contour, while inversely for the backward contour (see figure 2). The average $\langle\mathcal{T}_C \cdots\rangle$ denotes $\mathrm{Tr}\left\{\rho(0)\mathcal{T}_C \cdots \exp\left[-\frac{i}{\hbar}\int_C H_\gamma(t')dt'\right]\right\}/Z(\lambda, t)$. The equation of motion of the three point Green function on the contour $\langle\mathcal{T}_C c^\dagger_{k\rm L}(t')X(t)d(t_2)\rangle$ is given by

$$\left(i\frac{\partial}{\partial t'} - \epsilon_{k\rm L}\right)\langle\mathcal{T}_C c^\dagger_{k\rm L}(t')X(t)d(t_2)\rangle = t^*_{k\rm L}\langle\mathcal{T}_C d^\dagger(t')X^\dagger(t')X(t)d(t_2)\rangle \tag{16}$$

which can be written in the integral form [38]

$$\langle\mathcal{T}_C c^\dagger_{k\rm L}(t')X(t)d(t_2)\rangle = \int_C dt_1 \langle\mathcal{T}_C d^\dagger(t_1)X^\dagger(t_1)X(t)d(t_2)\rangle t^*_{k\rm L}g_{k\rm L}(t_1, t'). \tag{17}$$

Under DTA, one has the following decoupling [20]

$$\langle\mathcal{T}_C d^\dagger(t_1)X^\dagger(t_1)X(t)d(t_2)\rangle \simeq \langle\mathcal{T}_C X^\dagger(t_1)X(t)\rangle\langle\mathcal{T}_C d^\dagger(t_1)d(t_2)\rangle = \Lambda(t, t_1)G(t_2, t_1), \tag{18}$$

with $\Lambda(t, t_1) = \langle\mathcal{T}_C X^\dagger(t_1)X(t)\rangle$ being the phonon cloud propagator which will be discussed later. Then we have

$$t_{k\rm L}\langle\mathcal{T}_C c^\dagger_{k\rm L}(t')X(t')d(t')\rangle = \int_C dt_1 G(t', t_1)\Lambda(t', t_1)\Sigma(t_1, t'). \tag{19}$$

The self-energies due to the coupling to the leads under the DTA can be expressed as,

$$\Sigma^{ab}_{\alpha,D}(t_1, t_2) = \Sigma^{ab}_\alpha(t_1, t_2)\Lambda^{ba}_\alpha(t_2, t_1) = \Sigma^{ab}_\alpha(t_1, t_2)\Lambda^{ab}_\alpha(t_1, t_2), \tag{20}$$

where $a,\ b = +,-$ denote different Keldysh components and

$$\Sigma_{\alpha}^{ab}(t_1,\ t_2) = ab\theta(t_1)\theta(t_2)\sum_{k} t_{k\alpha}^{*} g_{k\alpha}^{ab}(t_1,\ t_2)t_{k\alpha}. \tag{21}$$

Note that the counting field enters the self-energy in the absence of the phonon cloud operator and the modified self-energy can be expressed by [34] $\widetilde{\Sigma}_{L}^{ab}(t_1,\ t_2) = \Sigma_{L}^{ab}(t_1 - t_2 - (a-b)\hbar\lambda)$. One can rewrite equation (15) as

$$\frac{\partial \ln Z}{\partial \lambda} = -\int_0^t dt_1 \int_0^t dt_2\, \mathrm{Tr}_K\left\{\frac{\partial \widetilde{\Sigma}_{\mathrm{L,D}}(t_1,\ t_2)}{\partial \lambda} G(t_2,\ t_1)\right\}, \tag{22}$$

where Tr_K indicates that the trace is over the Keldysh space. Using the fact that $Z(\lambda = 0,\ t) = 1$, the GF can be expressed in the Fredholm determinant by the Keldysh NEGF in the time domain as [19, 20],

$$Z(\lambda,\ t) = \det(G\widetilde{G}^{-1}) \tag{23}$$

with

$$G^{-1} = G_0^{-1} - \Sigma_{\mathrm{L,D}} - \Sigma_{\mathrm{R,D}}, \quad \widetilde{G}^{-1} = G_0^{-1} - \widetilde{\Sigma}_{\mathrm{L,D}} - \Sigma_{\mathrm{R,D}}, \tag{24}$$

where G_0 denotes the Green's function of the uncoupled QD, and the *tilde* indicates the inclusion of the counting field in the self-energy $\Sigma_{\alpha,D}$. Note that the Green's functions and self-energies without counting field possess the Keldysh structure,

$$A = \begin{pmatrix} A^{++} & A^{+-} \\ A^{-+} & A^{--} \end{pmatrix}. \tag{25}$$

The phonon cloud operator $\Lambda_{\delta}^{ab}(t_1,\ t_2)$ that is coupled to lead $\delta = \mathrm{L},\ \mathrm{R}$ is given by [7],

$$\Lambda_{\delta}^{+-}(t_1,\ t_2) = [\Lambda_{\delta}^{-+}(t_1,\ t_2)]^{*} = \sum_{m=-\infty}^{\infty} \alpha_{m\delta} e^{im\omega_0(t_1 - t_2)}, \tag{26}$$

with

$$\alpha_{m\delta} = e^{-g^2(2n_{B\delta}+1)} e^{m\beta_{\delta}\omega_0/2} I_m(2g^2\sqrt{n_{B\delta}(1+n_{B\delta})}), \tag{27}$$

and I_m being the modified Bessel function of the first kind, and Bose factor $n_{B\delta} = 1/(e^{\beta_{\delta}\omega_0} - 1)$, $\beta_{\delta} = 1/k_B T_{\delta}$. We should mention that the temperature of the phonon cloud operator is dependent on which self-energy it multiplies with, and in the next section we will see that this will ensure the important fluctuation symmetry relation. In the work by Utsumi *et al*, a third thermal probe electrode due to the thermal bath was added to determine the temperature of the vibrations [55]. In our work, we only consider the energy flow carried by electrons, and the fluctuation symmetry relation is already satisfied for the two-terminal system in equation (43). At zero temperature $\alpha_m = \alpha_{m\mathrm{L}} = \alpha_{m\mathrm{R}}$ can be simplified as,

$$\alpha_m = \begin{cases} e^{-g^2} g^{2m}/m! & \text{if } m \geqslant 0 \\ 0 & \text{if } m < 0 \end{cases}. \tag{28}$$

The remaining components of Λ_{δ} can be calculated by the relations,

$$\begin{aligned} \Lambda_{\delta}^{++}(t_1,\ t_2) &= \theta(t_1 - t_2)\Lambda_{\delta}^{-+}(t_1,\ t_2) + \theta(t_2 - t_1)\Lambda_{\delta}^{+-}(t_1,\ t_2), \\ \Lambda_{\delta}^{--}(t_1,\ t_2) &= \theta(t_2 - t_1)\Lambda_{\delta}^{-+}(t_1,\ t_2) + \theta(t_1 - t_2)\Lambda_{\delta}^{+-}(t_1,\ t_2). \end{aligned} \tag{29}$$

The Dyson equation bearing a Keldysh structure under DTA is

$$G = G_0 + G_0\Sigma_D G, \tag{30}$$

where $\Sigma_D = \Sigma_{\mathrm{L},D} + \Sigma_{\mathrm{R},D}$.

Utilizing the Dyson equation, equation (23) can be written as,

$$Z(\lambda,\ t) = \det[I - G(\widetilde{\Sigma}_{\mathrm{L},D} - \Sigma_{\mathrm{L},D})], \tag{31}$$

so that CGF has the form,

$$\ln Z(\lambda,\ t) = \mathrm{Tr}\ln[I - G(\widetilde{\Sigma}_{\mathrm{L},D} - \Sigma_{\mathrm{L},D})], \tag{32}$$

by using the relation $\det B = \exp[\mathrm{Tr}\ln B]$. Taking the first derivative of GF and noting that $\widetilde{\Sigma}_{\mathrm{L}}^{+-}(t_1,\ t_2) = -\sum_k t_{k\mathrm{L}}^{*} g_{k\mathrm{L}}^{+-}(t_1 - t_2 - \lambda)t_{k\mathrm{L}}$, energy current in the transient regime is found to be,

$$I_L^E(t) = \int_0^t dt'[G^{+-}(t,\ t')\breve{\Sigma}^{-+}(t',\ t) - G^{-+}(t,\ t')\breve{\Sigma}^{+-}(t',\ t)], \tag{33}$$

where

$$\breve{\Sigma}^{+-}(t',\,t) = -\Lambda^{+-}(t'-t)\sum_{k}\epsilon_{k\mathrm{L}}t^{*}_{k\mathrm{L}}g^{+-}_{k\mathrm{L}}(t'-t)t_{k\mathrm{L}}, \tag{34}$$

and we have a similar definition for $\breve{\Sigma}^{-+}(t',\,t)$. The transient current expression formally agrees with the one which was obtained directly by NEGF method [56].

3. Steady state energy transport FCS

In the long time limit, the system goes to steady state, and the Dyson equation equation (30) bearing the Keldysh structure in the energy domain can be expressed by

$$G = G_0 + G_0\Sigma_D G, \tag{35}$$

so that [18]

$$G = \frac{-1}{\mathcal{D}(\omega)}\begin{bmatrix} -(\omega-\bar{\epsilon})-\Sigma_D^{--} & \Sigma_D^{+-} \\ \Sigma_D^{-+} & (\omega-\bar{\epsilon})-\Sigma_D^{++}\end{bmatrix}, \tag{36}$$

with

$$\mathcal{D}(\omega) = [\omega-\bar{\epsilon}-\Sigma_D^{r}(\omega)][\omega-\bar{\epsilon}-\Sigma_D^{a}(\omega)]. \tag{37}$$

The dressed retarded self-energy in frequency domain was obtained by the Fourier transformation of the time domain counterpart with the form $\Sigma_D^r(t_1,\,t_2) = \theta(t_1-t_2)[\Sigma_D^{+-}(t_1,\,t_2)-\Sigma_D^{-+}(t_1,\,t_2)]$, so that in wide band limit (WBL) $W\to\infty$, [18]

$$\Sigma^r_{\alpha,D}(\omega) = \sum_m \alpha_m \int\frac{dE}{2\pi}\frac{\Gamma_\alpha[1+f_{\alpha+m}(E)-f_{\alpha-m}(E)]}{\omega-E+i0^+}. \tag{38}$$

The real and imaginary part was obtained using Plemelj formula $1/(E\pm i0^+) = P(1/E)\mp i\pi\delta(E)$ which will be used in the numerical calculation. One can verify that the real part and imaginary part satisfies

$$\mathrm{Im}\,[\Sigma^r_{\alpha,D}(\mu_\alpha+\omega)] = \mathrm{Im}\,[\Sigma^r_{\alpha,D}(\mu_\alpha-\omega)],\qquad \mathrm{Re}\,[\Sigma^r_{\alpha,D}(\mu_\alpha+\omega)] = -\mathrm{Re}\,[\Sigma^r_{\alpha,D}(\mu_\alpha-\omega)], \tag{39}$$

respectively [18].

In the long time limit, the Green's function and self-energy in equation (32) become time translation invariant so that scaled cumulant generating function (SCGF) $\mathcal{F}(\lambda) = \lim_{t\to\infty}\ln Z(\lambda)/t$ could be expressed in the energy domain as

$$\mathcal{F}(\lambda) = \int\frac{d\omega}{2\pi}\ln\left\{1+\sum_{mn}T_{mn}(\omega)[f_{\mathrm{L}+m}(1-f_{\mathrm{R}-n})(e^{i\lambda\omega}-1)+f_{\mathrm{R}+n}(1-f_{\mathrm{L}-m})(e^{-i\lambda\omega}-1)]\right\}. \tag{40}$$

In this expression $T_{mn}(\omega)$ is the transmission coefficient involving m and n vibrational quanta in the left and right lead, respectively, with the form,

$$T_{mn}(\omega) = \frac{\Gamma_{\mathrm{L}}\Gamma_{\mathrm{R}}\alpha_m\alpha_n}{\mathcal{D}(\omega)}. \tag{41}$$

Taking the first order derivative of SCGF with respect to λ, we obtained the expression of energy current,

$$\langle I^E\rangle = \int\frac{d\omega}{2\pi}\hbar\omega\sum_{mn}T_{mn}(\omega)[f_{\mathrm{L}+m}(1-f_{\mathrm{R}-n})-f_{\mathrm{R}+n}(1-f_{\mathrm{L}-m})]. \tag{42}$$

Now we consider the universal relations for energy current cumulants under finite temperature gradient with zero bias which is similar to the universal relation for particle current cumulants [57, 58]. Using the relation $\alpha_{-m} = e^{-\beta_{\mathrm{L}}m\omega_0}\alpha_m$, $\alpha_{-n} = e^{-\beta_{\mathrm{R}}n\omega_0}\alpha_n$ and $f_{\mathrm{R}}(1-f_{\mathrm{L}}) = \exp(\Delta\beta\omega)f_{\mathrm{L}}(1-f_{\mathrm{R}})$ with $\Delta\beta = \beta_{\mathrm{L}}-\beta_{\mathrm{R}}$ for $\Delta\mu = 0$ in equation (40), we obtain the fluctuation symmetry relation

$$\mathcal{F}(\xi) = \mathcal{F}(-\xi+\Delta\beta) \tag{43}$$

with $i\lambda$ being replaced by ξ for convenience. One can verify that the fluctuation symmetry can only be satisfied by considering the dependency of phonon temperature with respect to the specific lead. In the linear response regime $\Delta\beta\to 0$, we can expand both sides as Taylor series around $\Delta\beta = 0$ and $\xi = 0$, which leads to,

$$\left.\frac{d^k\mathcal{F}(-\xi+\Delta\beta,\,\Delta\beta)}{d\Delta\beta^k}\right|_0 = \left.\sum_{l=0}^{k}\binom{k}{l}\frac{\partial^k\mathcal{F}(\xi,\,\Delta\beta)}{\partial\Delta\beta^{k-l}\partial\xi^l}\right|_0, \tag{44}$$

where we have written the dependence of $\Delta\beta$ of SCGF explicitly out in both sides. Since $\mathcal{F}(\xi=0,\,\Delta\beta) = 0$, equation (43) gives $\mathcal{F}(\Delta\beta,\,\Delta\beta) = 0$, from which we find that the LHS of equation (44) vanishes. The last term

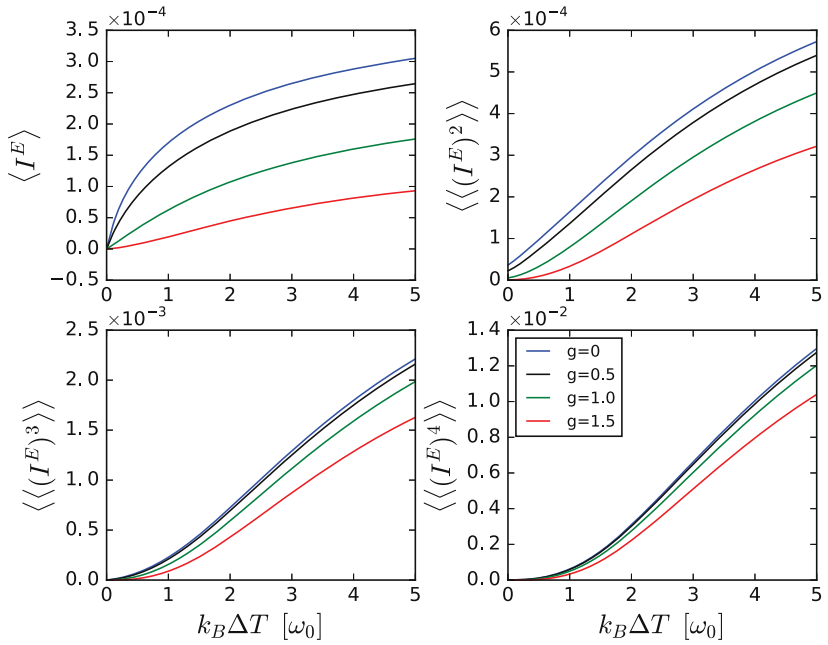

Figure 3. First to fourth energy current cumulants for increasing g (0 (blue), 0.5 (green), 1.0 (black) and 1.5 (red)) versus temperature gradient $\Delta T = T_{\rm L} - T_{\rm R}$ with the left lead warmer and temperature of right lead fixed at $k_B T_{\rm R} = 0.2\omega_0$. The renormalized energy level of the QD is $\bar{\epsilon} = 0$.

in the summation of equation (44) is the kth derivative of the SCGF with respect to the counting field ξ, which is actually $\langle\langle (I^E)^k \rangle\rangle$ at equilibrium. Then we have the relation

$$\langle\langle (I^E)^k \rangle\rangle_{\rm eq} = -\sum_{l=1}^{k-1} \binom{k}{l} \frac{\partial^{k-l} \langle\langle (I^E)^l \rangle\rangle}{\partial \Delta\beta^{k-l}}, \tag{45}$$

in which the energy current cumulant at equilibrium is expressed by a linear combination of lower order energy current cumulants. This is similar to the case where the particle current cumulant could be expressed by a linear combination of lower order particle current cumulants in the presence of small voltage bias [57, 58].

We now show the numerical calculations regarding steady state energy current cumulants under temperature gradient and external bias of molecular junctions in the polaronic regime. The energies are measured in the unit of vibron frequency ω_0, and the linewidth amplitude is chosen to be $\Gamma = 0.05\omega_0$ which indicates weak coupling. In addition, WBL is taken in our steady state calculation.

The first to fourth energy current cumulants for increasing g versus temperature gradient $\Delta T = T_{\rm L} - T_{\rm R}$ with the left lead warmer and temperature of right lead fixed at $k_B T_{\rm R} = 0.2\omega_0$ are shown in figure 3. The chemical potentials in both leads are set to be zero and the renormalized energy level of the QD is $\bar{\epsilon} = 0$. The energy current cumulants become smaller with the increasing of g because of the suppression of transport due to electron–phonon interaction. The second energy current cumulant with zero temperature gradient is finite due to the thermal noise in the leads, and it is reduced with increasing g.

In figure 4, energy current cumulants with different renormalized energy levels of the QD with $g = 1$ are plotted. We can see that the first to fourth cumulants and SCGF as well are even functions of $\bar{\epsilon}$. This can be understood as follows. Since the chemical potentials of both leads are zero, one can set

$$X_{mn}(\omega) = f_{{\rm L}+m}(\omega)[1 - f_{{\rm R}-n}(\omega)]e^{i\lambda\omega} + f_{{\rm R}+n}(\omega)[1 - f_{{\rm L}-m}(\omega)]e^{-i\lambda\omega}, \tag{46}$$

and verify that,

$$X_{mn}(\omega) = X_{mn}(-\omega), \tag{47}$$

using the relation $f_{{\rm L}+m}(\omega) = 1 - f_{{\rm L}-m}(-\omega)$. In the WBL, from equation (39), the real and imaginary part of the dressed retarded self-energy are the odd and even function of ω, respectively, so that we obtain the following symmetry with respect to the transmission coefficient in the polaronic regime

$$T_{mn}(\omega, \bar{\epsilon}) = T_{mn}(-\omega, -\bar{\epsilon}), \tag{48}$$

where the dependency of $\bar{\epsilon}$ has been written explicitly. Then, we have the following symmetry of SCGF with respect to $\bar{\epsilon}$,

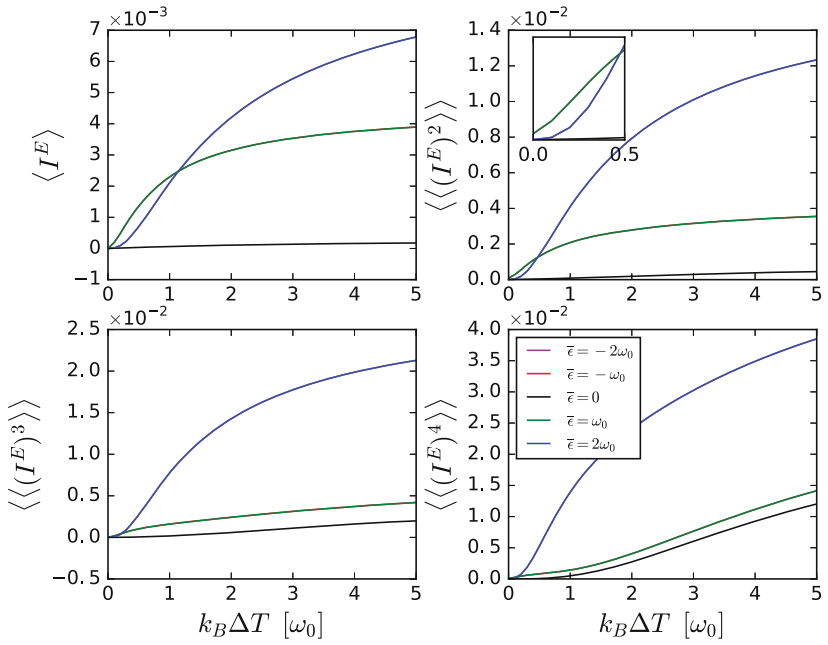

Figure 4. First to fourth energy current cumulants for different renormalized energy levels of the QD $\bar{\epsilon}$ ($-2\omega_0$ (magenta), $-\omega_0$ (red), 0 (black) ω_0 (green) and $2\omega_0$ (blue)) versus temperature gradient $\Delta T = T_L - T_R$ with $k_B T_R = 0.2\omega_0$. $g = 1.0$. First to fourth cumulants are even functions of $\bar{\epsilon}$. The lines of $\bar{\epsilon} = -2\omega_0$ coincide with the lines of $\bar{\epsilon} = 2\omega_0$, and the lines of $\bar{\epsilon} = -\omega_0$ coincide with the lines of $\bar{\epsilon} = \omega_0$.

$$\mathcal{F}(\lambda, \bar{\epsilon}) = \mathcal{F}(\lambda, -\bar{\epsilon}), \tag{49}$$

with $\mu_L = \mu_R = 0$ in the WBL. One can also see from figure 4 that $\langle I^E \rangle(\bar{\epsilon} = 2\omega_0)$ is smaller than $\langle I^E \rangle(\bar{\epsilon} = \omega_0)$ under small temperature gradient, and this is also true for the second energy current cumulant. Since the linewidth amplitude $\Gamma = 0.05\omega_0$ is small, the transmission coefficient which is centered around $\bar{\epsilon}$ is narrow. As a result, the main contribution to the transport process is coming from energy near $\bar{\epsilon}$. When the temperature gradient across the junction is small, the difference of Fermi distribution functions between the left and right leads $f_L(\omega) - f_R(\omega)$ is smaller near $\bar{\epsilon} = 2\omega_0$ than near $\bar{\epsilon} = \omega_0$. When T_L increases, the difference of Fermi distribution functions between left and right lead $f_L(\omega) - f_R(\omega)$ near $\omega = 2\omega_0$ can exceed the difference near $\omega = \omega_0$, so that the first and second cumulants with larger $\bar{\epsilon}$ are larger than the ones with smaller $\bar{\epsilon}$.

The first to fourth energy current cumulants for increasing g versus external bias $\Delta\mu$ with $\mu_L = \Delta\mu/2$ and $\mu_R = -\Delta\mu/2$ are shown in figure 5. The temperatures of both leads are chosen to be very small with $k_B T_L = k_B T_R = 0.04\omega_0$ which is almost in the regime of zero temperature. The renormalized energy level of the QD is $\bar{\epsilon} = 2\omega_0$. For the noninteracting case, the energy current and second cumulant are almost zero when the bias is below $\Delta\mu = 4\omega_0 = 2\bar{\epsilon}$ and display plateau structures when the external bias exceeds $2\bar{\epsilon}$. The width of transmission coefficient is small due to the small linewidth amplitude $\Gamma = 0.05\omega_0$. When $\Delta\mu = 2\bar{\epsilon}$, the chemical potential of the left lead is equal to the renormalized energy of QD, $\mu_L = \bar{\epsilon}$, in which energy the transmission coefficient experiences a sharp increase and reaches its largest value as indicated in figure 1(b). From figure 5, we observe that electron–phonon coupling enables the plateau height to become smaller, however, it creates smaller steps at $\Delta\mu = 2\bar{\epsilon} + 2n\omega_0$ with $n = 1, 2, 3\cdots$. This is due to the presence of sidebands in the leads and can be understood as follows. In the presence of the polaronic regime, from equation (42), we can approximately write the energy current in the presence of bias voltage at zero temperature as, (ignore the terms with product of Fermi distribution function)

$$\begin{aligned}\langle I^E \rangle \approx \int \frac{d\omega}{2\pi}\hbar\omega \sum_{m\geqslant 0} T_m(\omega)(f_{L+m} - f_{R+m}) = \int_{-\Delta\mu/2}^{\Delta\mu/2} \frac{d\omega}{2\pi}\hbar\omega T_0 \\ + \int_{-\Delta\mu/2-\omega_0}^{\Delta\mu/2-\omega_0} \frac{d\omega}{2\pi}\hbar\omega T_1 + \int_{-\Delta\mu/2-2\omega_0}^{\Delta\mu/2-2\omega_0} \frac{d\omega}{2\pi}\hbar\omega T_2 + \cdots,\end{aligned} \tag{50}$$

with $T_m = \frac{\Gamma_L \Gamma_R \alpha_m}{\mathcal{D}(\omega)} \propto \alpha_m = e^{-g^2} g^{2m}/m!$. The energy current is written as a sum of a series, with each term coming from a different sideband in the leads. The first plateau of the energy current in the polaronic regime is mainly due to the first term in equation (50), and the second plateau due to the contribution from the second term in equation (50) with one polaron involved in the transport process, etc. We find that $T_m/T_{m-1} = g^2/m$ is responsible for the ratios between plateau heights. One can see that when $g = 0.5$, $T_1/T_0 = 0.25$, the height of the second plateau is a quarter of that of the first plateau at zero temperature, which explains what we see in

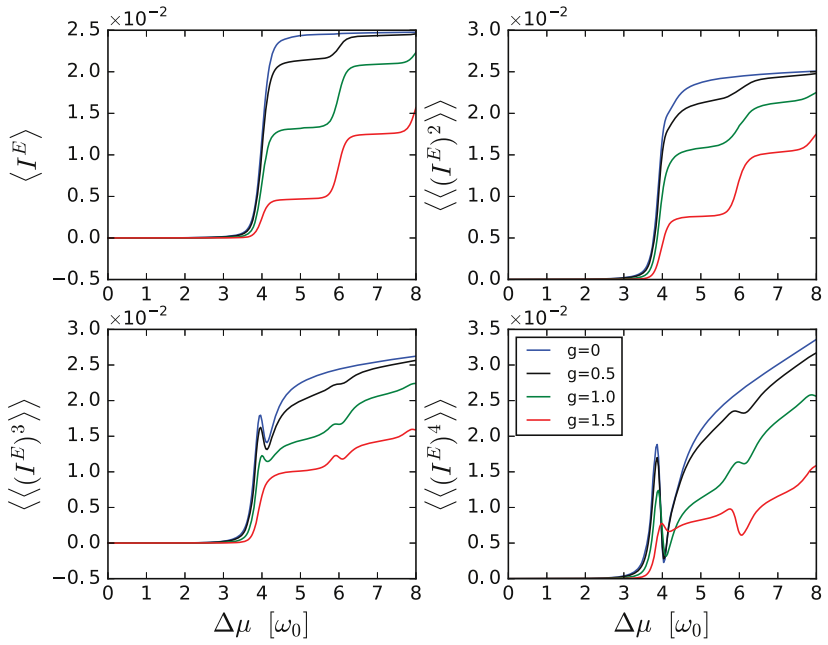

Figure 5. First to fourth energy current cumulants for increasing g (0 (blue), 0.5 (green), 1.0 (black) and 1.5 (red)) versus external bias $\Delta\mu$ with $\mu_L = \Delta\mu/2$ and $\mu_R = -\Delta\mu/2$. The temperatures of both leads are $k_B T_L = k_B T_R = 0.04\omega_0$. The renormalized energy level of the QD is chosen to be $\bar{\epsilon} = 2\omega_0$.

figure 5. This is also applicable to the case of $g = 1.0$ with $T_1/T_0 = 1.0$ and the case of $g = 1.5$ with $T_1/T_0 = 2.25$. One should note that the temperature of the system in figure 5 is very small.

The plateau structures disappear in the third and fourth energy current cumulants. Instead a dip occurs at $\Delta\mu = 2\bar{\epsilon}$ for both the third and fourth energy current cumulants with the fourth cumulant larger for both the noninteracting and interacting cases. The polaronic regime creates smaller dips at $\Delta\mu = 2\bar{\epsilon} + 2n\omega_0$ with $n = 1, 2, 3\cdots$ which can also be identified in figure 7. Increasing g reduces the amplitude of the dip at $\Delta\mu = 2\bar{\epsilon}$ but increases the amplitude at $\Delta\mu = 2\bar{\epsilon} + 2n\omega_0$. The explanation is as follows. For the noninteracting case under zero temperature, we have

$$\begin{aligned}
\langle I^E \rangle &= \int \frac{d\omega}{2\pi} \omega T(\omega), \quad \langle\langle (I^E)^2 \rangle\rangle = \int \frac{d\omega}{2\pi} \omega^2 T(\omega)[1 - T(\omega)], \\
\langle\langle (I^E)^3 \rangle\rangle &= \int \frac{d\omega}{2\pi} \omega^3 T(\omega)[1 - T(\omega)][1 - 2T(\omega)], \\
\langle\langle (I^E)^4 \rangle\rangle &= \int \frac{d\omega}{2\pi} \omega^4 T(\omega)[1 - T(\omega)][1 - 6T(\omega) + 6T^2(\omega)],
\end{aligned} \tag{51}$$

with the ranges of integration from $-\Delta\mu/2$ to $\Delta\mu/2$. We can further take derivative of $\langle\langle (I^E)^k \rangle\rangle$ with respect to external bias $\Delta\mu$, $\partial\langle I^E \rangle/\partial\Delta\mu$ and $\partial\langle\langle (I^E)^2 \rangle\rangle/\partial\Delta\mu$ as always being positive definite since the transmission coefficient for the noninteracting case has the form $T(\omega) = \frac{\Gamma^2/4}{(\omega - \bar{\epsilon})^2 + \Gamma^2/4}$. However the derivative of the third and fourth cumulants with respect to the external bias change sign around $\Delta\mu = 2\bar{\epsilon}$ and also the transmission coefficient experiences an abrupt change because of small linewidth amplitude. This leads to the the dips of the third and forth cumulants of energy current as shown in figure 5.

The influence of temperature on cumulants under external bias is depicted in figure 6, and one can see that both the plateaus and dips get smoothed or even disappear when temperature increases. In figure 7, energy current cumulants with different $\bar{\epsilon}$ with $g = 1$ are plotted. We can see that the first and third cumulants are odd functions of $\bar{\epsilon}$, while the second and fourth cumulants are even functions of $\bar{\epsilon}$. The reason is as follows. Under zero temperature, the transport is unidirectional and the Fermi–Dirac distribution function $f_{L(R)}$ has a step-wise form, since the transmission coefficient is peaked around the resonant level $\bar{\epsilon}$ with a very small linewidth amplitude (say $\delta\epsilon$), the energies carried by electrons which mainly contribute to energy transport are very close to $\bar{\epsilon}$. So if we change the sign of $\bar{\epsilon}$ from positive to negative, then most of the electron energies will reverse their signs if $\delta\epsilon < \bar{\epsilon}$. Since the energy current is proportional to the energies carried by electrons, this will lead to the reversal of the energy current.

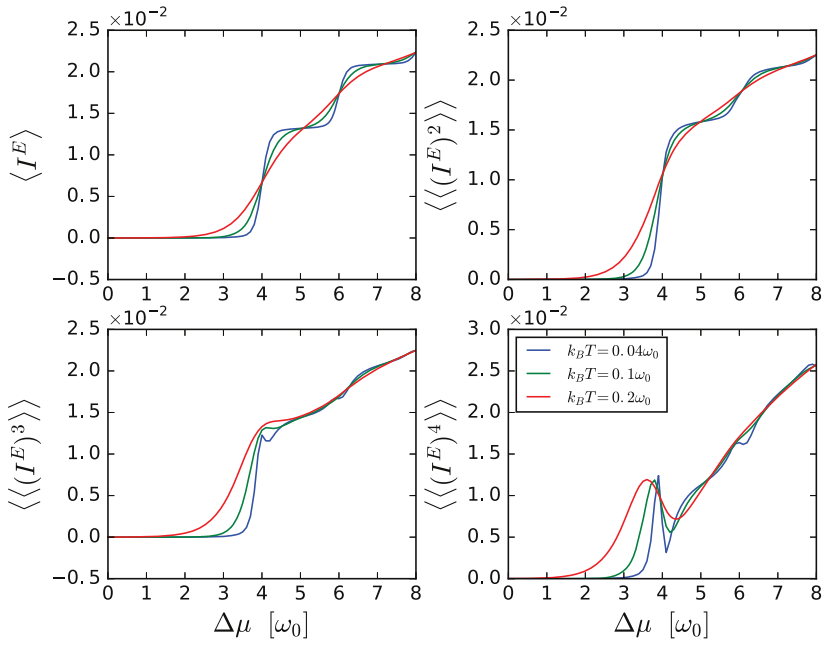

Figure 6. First to fourth energy current cumulants for increasing temperatures k_{BT} ($0.04\omega_0$ (blue), $0.1\omega_0$ (green) and $0.2\omega_0$ (red)) versus external bias $\Delta\mu$ with $\mu_{L(R)} = \pm\Delta\mu/2$. $g = 1.0$ and $\bar{\epsilon} = 2\omega_0$.

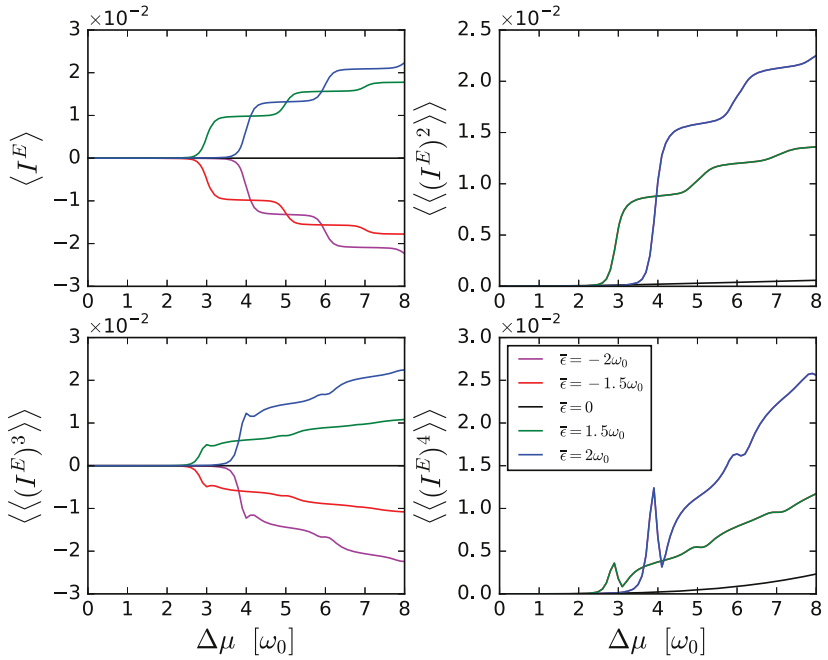

Figure 7. First to fourth energy current cumulants for different $\bar{\epsilon}$ ($-2\omega_0$ (magenta), $-1.5\omega_0$ (red), 0 (black) $1.5\omega_0$ (green) and $2\omega_0$ (blue)) versus external bias $\Delta\mu$ with $\mu_L = \Delta\mu/2$ and $\mu_R = -\Delta\mu/2$. $g = 1.0$ and the temperatures of both leads are $k_B T_L = k_B T_R = 0.04\omega_0$. The lines of the second and fourth cumulants of $\bar{\epsilon} = -2\omega_0$ coincide with the lines of $\bar{\epsilon} = 2\omega_0$, and the lines of the second and fourth cumulants of $\bar{\epsilon} = -\omega_0$ coincide with the lines of $\bar{\epsilon} = \omega_0$.

4. Transient dynamics of energy transport

We first investigate the behaviors of energy current at a very short time limit. To do that, we expand the GF to the lowest order in time,

$$Z(\lambda, t) \approx 1 + \int_0^t dt_1 \int_0^t dt_2 [\widetilde{\Sigma}^{-+}_{\mathrm{L},D}(t_1, t_2) - \Sigma^{-+}_{\mathrm{L},D}(t_1, t_2)] G_0^{+-}(t_2, t_1) + [\widetilde{\Sigma}^{+-}_{\mathrm{L},D}(t_1, t_2) - \Sigma^{+-}_{\mathrm{L},D}(t_1, t_2)] G_0^{-+}(t_2, t_1). \quad (52)$$

The expressions of the Green's function for isolated QD and self-energy are given in the appendix. Under the wide band limit $W \to \infty$, we can obtain the GF in the short time limit in a compact form as,

$$Z(\lambda, t) \approx 1 + A_{\mathrm{L}0}(n_d - 1) + A_{\mathrm{L}1} n_d, \quad (53)$$

where

$$A_{\mathrm{L}0} = \frac{\Gamma_{\mathrm{L}}}{\pi} \sum_{n=-\infty}^{\infty} \alpha_n \int d\omega (e^{i\omega\lambda} - 1) M(\omega) f_{\mathrm{L}+n}(\omega),$$
$$A_{\mathrm{L}1} = \frac{\Gamma_{\mathrm{L}}}{\pi} \sum_{n=-\infty}^{\infty} \alpha_n \int d\omega (e^{-i\omega\lambda} - 1) M(\omega) [f_{\mathrm{L}-n}(\omega) - 1], \quad (54)$$

with

$$M(\omega) = \frac{1 - \cos[(\omega - \bar{\epsilon})t]}{(\omega - \bar{\epsilon})^2}. \quad (55)$$

From here on we use $f_{\alpha\pm n}$ to denote $f_\alpha(\omega \pm n\omega_0)$. We can see from the expression of the short time limit of the GF that the transport process is unidirectional in the short time limit. We obtain the current expressions in the short time limit as

$$I^E_{\mathrm{L}}(t) = \frac{d}{dt} \frac{\partial \ln Z(\lambda, t)}{\partial(i\lambda)} \bigg|_{\lambda=0} = \frac{\Gamma_{\mathrm{L}}}{\pi} \sum_{n=-\infty}^{\infty} \alpha_n \int d\omega \frac{\omega \sin[(\omega - \bar{\epsilon})t]}{\omega - \bar{\epsilon}} \{f_{\mathrm{L}+n}(\omega)(n_d - 1) - [f_{\mathrm{L}-n}(\omega) - 1] n_d\}. \quad (56)$$

We apply the formalism to perform numerical calculation with respect to the transient dynamics of energy current under temperature gradient and external bias, respectively. The energies are measured in the unit of Γ and $1/\Gamma$ is the unit of time. We only consider the case where the QD is initially unoccupied $n_d = 0$ and the linewidth amplitude in equation (5) is set to be $\Gamma_{\mathrm{L}} = \Gamma_{\mathrm{R}} = \Gamma/2$ and the bandwidth is also set to be the same for both leads with $W = 10\Gamma$.

The first to fourth transient energy current cumulants, $\langle\langle (I^E)^k \rangle\rangle$ for $k = 1, 2, 3, 4$, in the left lead for increasing g under temperature gradient and external bias are shown, respectively, in figure 8 and in figure 9. Increasing g corresponds to the increasing of the electron–phonon coupling strength. The frequency of the localized vibron is $\omega_0 = 6\Gamma$. The renormalized energy level of the QD is $\bar{\epsilon} = 2\Gamma$ for case under temperature gradient and $\bar{\epsilon} = 1.5\Gamma$ for the case with external bias. The left lead is assumed to be warmer with the temperatures of the two leads at $k_B T_{\mathrm{L}} = 1.5\Gamma$ and $k_B T_{\mathrm{R}} = 1.2\Gamma$ while the chemical potentials in both leads are set to zero in the case under temperature gradient. The temperature parameter in the phonon cloud operator equation (26) should be the temperature of the lead where the phonon cloud operator acts. For the case under external bias, the chemical potential of the left and right leads are chosen to be $\mu_{\mathrm{L}} = 2\Gamma$ and $\mu_{\mathrm{R}} = -2\Gamma$. The temperatures of both leads is zero, while a small temperature $k_B T = 0.1\Gamma$ in the phonon cloud operator is taken in order to stabilize the numerical calculations.

As a general feature for both the noninteracting ($g = 0$) and interacting cases, the transient amplitudes of $\langle\langle (I^E)^k \rangle\rangle$ increase with cumulants order. This behavior is universal and will be investigated in detail in figure 10. The second and fourth energy current cumulants may even oscillate to negative values at short time limits. The negativity of the second energy current cumulants can be explained as follows. The energy cumulant $C_2(t)$ must be positive at all times from a statistical view, however it can oscillate at short time limits so that the second energy current cumulant which is the derivative of $C_2(t)$ may not be positive at short time limits. $\langle\langle (I^E)^2 \rangle\rangle$ at steady state (long time limit) is positive and can be identified from the figures. The amplitudes of oscillation in the evolution and the asymptotic values of the cumulants are suppressed with the increasing of g. The first and third energy current cumulants in the stationary limit are positive under temperature and external bias, since we put the normalized energy level of QD above the Fermi energy of the both leads so that the electrons with positive energy contribute to the transport process. However, at short time limits, the energy current and third cumulant oscillate to negative values with a minimum. This can be understood as follows. Since the QD is prepared initially empty, once the system is connected, the contribution to the transport process mainly comes from electron of the left lead which can be seen from equation (53). The contribution of energy current cumulants from the energy window $[0, \mu_L]$ cancels with the contribution from $[-\mu_L, 0]$, so that energy below $-\mu_L$ in the left lead will contribute to the energy transport process which leads to the negativity of the first and third energy current cumulants in the short time limit. The cumulants of transient energy current approach to their steady state values in the long time limit.

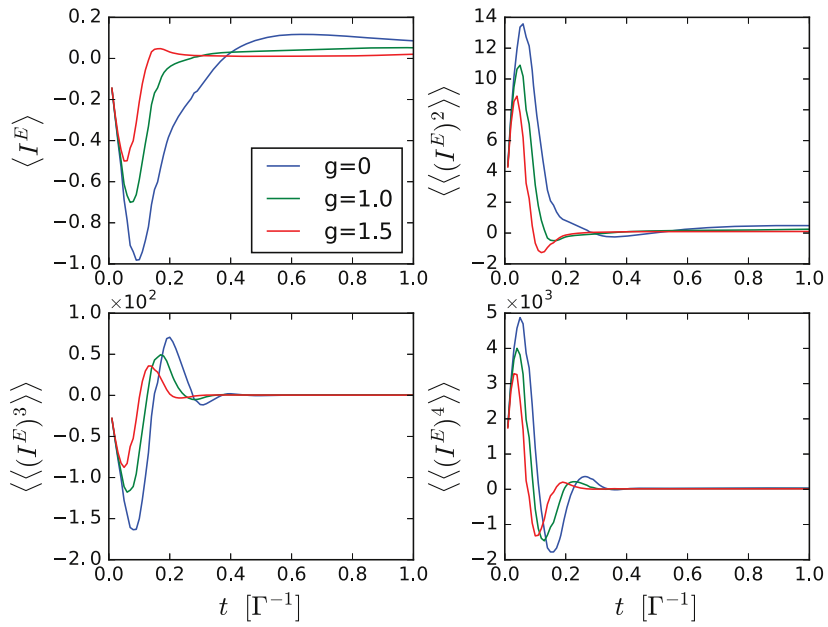

Figure 8. First to fourth transient energy current cumulants in the left lead for increasing g (0 (blue), 1.0 (green) and 1.5 (red)) for initially empty QD under temperature gradient between the leads. The energies are measured in the unit of Γ and $1/\Gamma$ is the unit of time. The temperatures of the two leads are chosen to be $k_B T_L = 1.5\Gamma$ and $k_B T_R = 1.2\Gamma$ with the left lead warmer. The renormalized energy level of the QD is $\bar{\epsilon} = 2\Gamma$ and the frequency of the localized vibron $\omega_0 = 6\Gamma$.

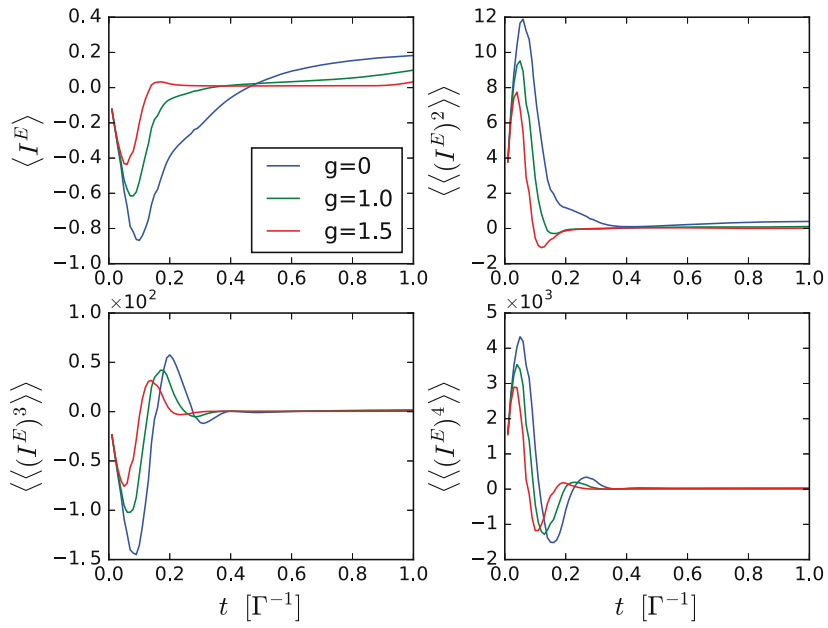

Figure 9. First to fourth transient energy current cumulants in the left lead for increasing g (0 (blue), 1.0 (green) and 1.5 (red)) for initially empty QD under external bias at zero temperature. The energies are measured in the unit of Γ and $1/\Gamma$ is the unit of time. The chemical potential of the left and right lead are chosen to be $\mu_{L(R)} = \pm 2\Gamma$. The renormalized energy level of the QD is $\bar{\epsilon} = 1.5\Gamma$ and the frequency of the localized vibron $\omega_0 = 6\Gamma$.

We also plot the logarithm of the maximum amplitude of the normalized transient energy cumulants $M_k = \max|C_k/C_1|$ under temperature gradient (figure 10(a)) and external bias (figure 10(b)). Different lines with respect to different bandwidths W are plotted, while the other parameters are same as in figures 8 and 9. The maximum amplitudes M_k for different interaction parameter $g = 0,\ 1.0$ and 1.5 coincide. We can see from the figure that both $\ln(M_{2k})$ and $\ln(M_{2k+1})$ are linear with cumulants order k with the slope close to 3 but they have different intercepts. This universal scaling of normalized transient energy cumulants is found under both the temperature gradient and external bias, and it is the result of the universality of the GF in the short time limit which has also been reported in charge cumulants [20, 59]. A theoretical understanding of this behavior for the

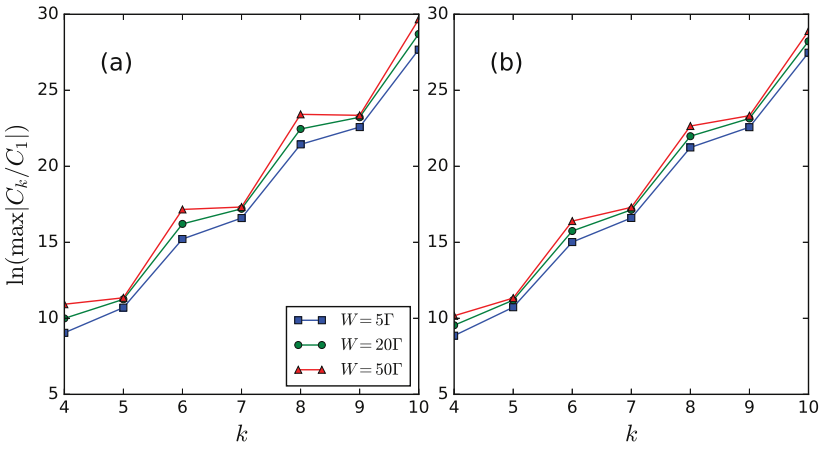

Figure 10. Logarithm of the maximum amplitude of the normalized transient energy cumulants $M_k = \max|C_k/C_1|$ at the short time limit versus k for different bandwidths W under (a) temperature gradient, and (b) external bias. Maximum amplitudes M_k for different interaction parameters $g = 0,\ 1.0$ and 1.5 coincide.

noninteracting case was reported in our previous work [34]. Interestingly, turning on the electron–phonon interaction does not affect this behavior.

5. Conclusion

Both the steady state and transient behaviors of energy transport carried by electrons in molecular junctions for the Anderson–Holstein model in the polaronic regime have been investigated using FCS. Using a two time measurement scheme and equation of motion technique, the GF for the energy current can be expressed as a Fredholm determinant in the time domain using NEGF. The DTA decoupling scheme [17] which can provide a good description of dealing with the phonon cloud operator has been adapted in obtaining the GF. This formalism allows us to analyze the time evolution of the energy transport dynamics after a sudden switch of the coupling between the dot and the leads towards the stationary state. The amplitudes of the oscillation in the evolution and the asymptotic values of the cumulants are suppressed with the increasing of g. The universal scaling of normalized transient energy cumulants is found under external bias.

In the steady states, universal relations for energy current cumulants under a finite temperature gradient with zero voltage bias and this enables us to express the equilibrium energy current cumulant by a linear combination of lower order cumulants. The behaviors of the energy current cumulants (from the first to the fourth) under temperature gradient and external bias are numerically shown and explained. Under external bias, the energy current and second cumulant are almost zero when the bias is below $\Delta\mu = 2\bar{\epsilon}$ for the noninteracting case and display plateau structures when the external bias exceeds $2\bar{\epsilon}$. Due to the sidebands in the leads in the polaronic regime, the plateau heights become smaller, however, smaller plateau steps appear at $\Delta\mu = 2\bar{\epsilon} + 2n\omega_0$ with $n = 1,\ 2,\ 3\cdots$. The plateau structures disappear in the third and fourth energy current cumulants. Instead a dip occurs at $\Delta\mu = 2\bar{\epsilon}$ for both the third and fourth energy current cumulants with the fourth cumulant larger for both the noninteracting and interacting cases. The polaronic regime creates smaller dips at $\Delta\mu = 2\bar{\epsilon} + 2n\omega_0$ with $n = 1,\ 2,\ 3\cdots$.

Acknowledgments

This work was financially supported by NSF-China under Grant No. 11374246, the General Research Fund (Grant No. 17311116), and the University Grant Council (Contract No. AoE/P-04/08) of the Government of HKSAR.

Appendix. Green's function and self-energy in the time domain

A description on how to calculate the uncoupled dot Green's function and the self-energy in the time domain in the absence of the phonon cloud operator is presented here. The four correlation functions of the uncoupled dot are given in a book written by Kamenev [40] as

$$
\begin{aligned}
iG_0^{+-}(t_1, t_2) &= -n_d \exp\{-i\bar{\epsilon}(t_1 - t_2)\} \\
iG_0^{-+}(t_1, t_2) &= (1 - n_d)\exp\{-i\bar{\epsilon}(t_1 - t_2)\} \\
iG_0^{++}(t_1, t_2) &= \theta(t_1 - t_2)iG_0^{-+} + \theta(t_2 - t_1)iG_0^{+-} \\
iG_0^{--}(t_1, t_2) &= \theta(t_2 - t_1)iG_0^{-+} + \theta(t_1 - t_2)iG_0^{+-},
\end{aligned} \tag{57}
$$

where n_d is the initial occupation number of the QD before the system is connected. The Lorentzian linewidth function with the linewidth amplitude Γ_α and bandwidth W,

$$
\mathbf{\Gamma}_\alpha(\omega) = \frac{\Gamma_\alpha W^2}{\omega^2 + W^2}, \tag{58}
$$

is used to describe the self-energy $\Sigma_{L(R)}$ in absence of the phonon cloud operator, so that the numerical calculation would be more realistic. The equilibrium energy dependent self-energy can be written as,

$$
\Sigma_\alpha^r(\omega) = \frac{\Gamma_\alpha W}{2(\omega + iW)}. \tag{59}
$$

Performing Fourier transform, the retarded self-energy in the time domain can be obtained [33],

$$
\Sigma_\alpha^r(t_1, t_2) = -\frac{i}{2}\theta(t_1 - t_2)\Gamma_\alpha W e^{-(i\mu_\alpha + W)(t_1 - t_2)}, \tag{60}
$$

where μ_α is the chemical potential of the α-lead. For the lower self-energy in the time domain,

$$
\Sigma_\alpha^<(t_1, t_2) = i\int \frac{d\omega}{2\pi} e^{-i\omega(t_1 - t_2)} f_\alpha(\omega)\mathbf{\Gamma}_L(\omega - \mu_\alpha) \tag{61}
$$

with $f_\alpha(\omega) = 1/[e^{\beta(\omega - \mu_\alpha)} + 1]$. It is a function of the time difference, and one can let $\tau = t_1 - t_2$ for convenience. When $t_1 = t_2$,

$$
\Sigma_\alpha^<(t_1, t_2) = \frac{i}{4}\Gamma_\alpha W. \tag{62}
$$

The case of $t_1 > t_2$ for both the zero and non-zero temperatures is to be considered first. At non-zero temperature, if $t_1 > t_2$, it has poles $\frac{-i(2n+1)\pi}{\beta_\alpha}$ and $-iW$, where $n = 0, 1, 2, 3$ ..., so that,

$$
\begin{aligned}
\Sigma_\alpha^<(t_1, t_2) &= \frac{i\Gamma_\alpha W}{2} e^{-i\mu_\alpha \tau}\left\{ e^{-W\tau}\left[1 + \frac{E1(-W\tau)}{2i\pi}\right] - e^{W\tau}\frac{E1(W\tau)}{2i\pi}\right\} \qquad k_B T_\alpha = 0, \\
\Sigma_\alpha^<(t_1, t_2) &= \frac{i\Gamma_\alpha W}{2} e^{-i\mu_\alpha \tau}\left\{ \frac{\exp(-W\tau)}{\exp(-i\beta_\alpha W) + 1} - \frac{2}{i\beta_\alpha}\sum_{n=0}^{+\infty} \exp\left[-\frac{(2n+1)\pi}{\beta_\alpha}\tau\right]\right. \\
&\quad \left. \times \frac{W}{W^2 - \left[\frac{(2n+1)\pi}{\beta_\alpha}\right]^2}\right\} \qquad k_B T_\alpha \neq 0,
\end{aligned} \tag{63}
$$

where $E1(x) = \int_x^\infty \frac{e^{-t}}{t} dt$. Using the relation $\Sigma_\alpha^<(t_1, t_2)|_{t_1 < t_2} = -[\Sigma_\alpha^<(t_1, t_2)|_{t_1 > t_2}]^*$, the full expression of $\Sigma_\alpha^<(t_1, t_2)$ can be obtained. The remaining components can be calculated by the relations,

$$
\begin{aligned}
\Sigma_\alpha^>(t_1, t_2) &= \Sigma_\alpha^<(t_1, t_2) + \Sigma_\alpha^r(t_1, t_2) - \Sigma_\alpha^a(t_1, t_2), \\
\Sigma_\alpha^t(t_1, t_2) &= \theta(t_1 - t_2)\Sigma_\alpha^>(t_1 - t_2) + \theta(t_2 - t_1)\Sigma_\alpha^<(t_1 - t_2), \\
\Sigma_\alpha^{\bar{t}}(t_1, t_2) &= \theta(t_2 - t_1)\Sigma_\alpha^>(t_1 - t_2) + \theta(t_1 - t_2)\Sigma_\alpha^<(t_1 - t_2).
\end{aligned} \tag{64}
$$

Note that the following relations hold $\Sigma_\alpha^{++} = \Sigma_\alpha^t$, $\Sigma_\alpha^{+-} = -\Sigma_\alpha^<$, $\Sigma_\alpha^{-+} = -\Sigma_\alpha^>$, and $\Sigma_\alpha^{--} = \Sigma_\alpha^{\bar{t}}$.

References

[1] Reichert J, Ochs R, Beckmann D, Weber H B, Mayor M and Löhneysen H V 2002 *Phys. Rev. Lett.* **88** 176804
[2] Liang W, Shores M, Bockrath M, Long J and Park H 2002 *Nature* **417** 725
[3] Ortmann F, Bechstedt F and Hannewald K 2009 *Phys. Rev.* B **79** 235206
[4] Ortmann F and Roche S 2011 *Phys. Rev.* B **84** 180302
[5] Koch J, von Oppen F and Andreev A V 2006 *Phys. Rev.* B **74** 205438
[6] Holstein T 1959 *Ann. Phys. (NY)* **8** 343
[7] Mahan G D 2000 *Many-Particle Physics* 3rd edn (Boston, MA: Springer)
[8] Koch J and von Oppen F 2005 *Phys. Rev. Lett.* **94** 206804
[9] Koch J, Raikh M E and von Oppen F 2005 *Phys. Rev. Lett.* **95** 056801
[10] Zazunov A, Feinberg D and Martin T 2006 *Phys. Rev.* B **73** 115405
[11] Shen X Y, Dong B, Lei X L and Horing N J M 2007 *Phys. Rev.* B **76** 115308
[12] Mühlbacher L and Rabani E 2008 *Phys. Rev. Lett.* **100** 176403
[13] Jovchev A and Anders F B 2013 *Phys. Rev.* B **87** 195112

[14] Ueda A and Eto M 2006 *Phys. Rev.* B **73** 235353
[15] Entin-Wohlman O, Imry Y and Aharony A 2010 *Phys. Rev.* B **81** 113408
[16] Utsumi Y, Entin-Wohlman O, Ueda A and Aharony A 2013 *Phys. Rev.* B **87** 115407
[17] Seoane Souto R, Levy Yeyati A, Martn-Rodero A and Monreal R C 2014 *Phys. Rev.* B **89** 085412
[18] Dong B, Ding G H and Lei X L 2013 *Phys. Rev.* B **88** 075414
[19] Dong B, Ding G H and Lei X L 2017 *Phys. Rev.* B **95** 035409
[20] Souto R S, Avriller R, Monreal R C, Martín-Rodero A and Yeyati A L 2015 *Phys. Rev.* B **92** 125435
[21] Blanter Y and Büttiker M 2000 *Phys. Rep.* **336** 1
[22] Levitov L S and Lesovik G B 1993 *Pisma Zh. Eksp. Teor. Fiz.* **58** 225
Levitov L S and Lesovik G B 1993 *Sov. Phys. JETP* **58** 230
[23] Levitov L S, Lee H-W and Lesovik G B 1996 *J. Math. Phys.* **37** 4845
[24] Levitov L S 2003 *Quantum Noise in Mesoscopic Physics, NATO Science Series II, Vol. 97* ed Y V Nazarov (Dordrecht: Kluwer)
[25] Klich I 2003 *Quantum Noise in Mesoscopic Physics, NATO Science Series II, Vol. 97* ed Y V Nazarov (Dordrecht: Kluwer)
[26] Nazarov Y V and Kindermann M 2003 *Eur. Phys. J.* B **35** 413–20
[27] Esposito M, Harbola U and Mukamel S 2009 *Rev. Mod. Phys.* **81** 1665
[28] Hassler F, Suslov M V, Graf G M, Lebedev M V, Lesovik G B and Blatter G 2008 *Phys. Rev.* B **78** 165330
[29] Wang J-S, Agarwalla B K and Li H 2011 *Phys. Rev.* B **84** 153412
[30] Agarwalla B K, Li B and Wang J-S 2012 *Phys. Rev.* E **85** 051142
[31] Agarwalla B K, Li H, Li B and Wang J-S 2014 *Phys. Rev.* E **89** 052101
[32] Tang G-M, Xu F and Wang J 2014 *Phys. Rev.* B **89** 205310
[33] Tang G-M and Wang J 2014 *Phys. Rev.* B **90** 195422
[34] Yu Z, Tang G-M and Wang J 2016 *Phys. Rev.* B **93** 195419
[35] Yuan J, Xing Y, Zhang L and Wang J 2017 *Phys. Rev.* B **95** 155402
[36] Tang G, Chen X, Ren J and Wang J arXiv:1705.10025
[37] Keldysh L V 1964 *Zh. Eksp. Teor. Fiz.* **47** 1515
Keldysh L V 1965 *Sov. Phys. JETP* **20** 1018
[38] Haug H and Jauho A-P 1998 *Quantum Kinetics in Transport and Optics of Semiconductors* (Berlin: Springer)
[39] Kamenev A 2002 *Strongly Correlated Fermions and Bosons in Low-Dimensional Disordered Systems, NATO Science Series II, Vol. 72* ed I V Lerner *et al* (Dordrecht: Kluwer)
[40] Kamenev A 2011 *Field Theory of Non-Equilibrium Systems* (Cambridge: Cambridge University Press)
[41] Campisi M, Hänggi P and Talkner P 2011 *Rev. Mod. Phys.* **83** 771
[42] Campisi M, Talkner P and Hänggi P 2011 *Phys. Rev.* E **83** 041114
[43] Campisi M, Talkner P and Hänggi P 2010 *Phys. Rev. Lett.* **105** 140601
[44] Schmidt T L and Komnik A 2009 *Phys. Rev.* B **80** 041307(R)
[45] Riwar R-P and Schmidt T L 2009 *Phys. Rev.* B **80** 125109
[46] Maier S, Schmidt T L and Komnik A 2011 *Phys. Rev.* B **83** 085401
[47] Sivan U and Imry Y 1986 *Phys. Rev.* B **33** 551
[48] Kearney M J and Butcher P N 1988 *J. Phys.* C **21** L265
[49] Buttiker M 1992 *Phys. Rev.* B **46** 12485
[50] Ramm M, Pruttivarasin T and Häffner H 2014 *New J. Phys.* **16** 063062
[51] Sothmann B, Sánchez R, Jordan A N and Büttiker M 2012 *Phys. Rev.* B **85** 205301
[52] Egger R and Gogolin A O 2008 *Phys. Rev.* B **77** 113405
[53] Lang I G and Firsov Y A 1963 *JETP* **16** 1301
[54] Komnik A and Gogolin A O 2005 *Phys. Rev. Lett.* **94** 216601
Gogolin A O and Komnik A 2006 *Phys. Rev.* B **73** 195301
[55] Utsumi Y, Entin-Wohlman O, Aharony A, Kubo T and Tokura Y 2014 Fluctuation theorem for heat transport probed by a thermal probe electrode *Phys. Rev.* **89** 205314
[56] Yu Z, Zhang L, Xing Y and Wang J 2014 *Phys. Rev.* B **90** 115428
[57] Tobiska J and Nazarov Y V 2005 *Phys. Rev.* B **72** 235328
[58] Förster H and Büttiker M 2008 *Phys. Rev. Lett.* **101** 136805
[59] Flindt C, Fricke C, Hohls F, Novotný T, Netočný K, Brandes T and Haug R J 2009 *Proc. Natl. Acad. Sci.* **106** 10116